NANO LETTERS
Letter
pubs.acs.org/NanoLett

Strain Paint: Noncontact Strain Measurement Using Single-Walled Carbon Nanotube Composite Coatings

Paul A. Withey,[†,‡,∥] Venkata Srivishnu M. Vemuru,[§,∥] Sergei M. Bachilo,[‡,∥] Satish Nagarajaiah,[§,∥] and R. Bruce Weisman*[,‡,∥]

[†]Department of Physics, University of Houston - Clear Lake, 2700 Bay Area Boulevard, Houston, Texas 77058, United States
[‡]Department of Chemistry, [§]Department of Mechanical Engineering and Materials Science, and Department of Civil and Environmental Engineering, and [∥]R.E. Smalley Institute for Nanoscale Science and Technology, Rice University, 6100 Main Street, Houston, Texas 77005, United States

ABSTRACT: Composite coatings have been developed that reveal strains in underlying structural elements through noncontact optical measurement. Dilute individualized single-walled carbon nanotubes are embedded in a polymeric host and applied to form a thin coating. Strain in the substrate is transmitted through the polymer to the nanotubes, causing systematic and predictable spectral shifts of the nanotube near-infrared fluorescence peaks. This new method allows quick and precise strain measurements at any position and along any direction of the substrate.

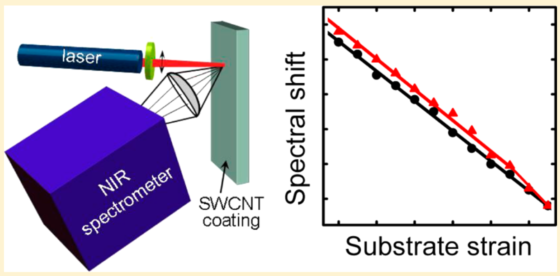

KEYWORDS: *SWCNT, fluorescence shifts, photoluminescence spectroscopy, structural health monitoring*

Operational safety of aircraft, bridges, and buildings requires periodic strain monitoring of key structural elements to prevent catastrophic failures. Existing methods for measuring strain involve implanted macroscopic sensors that report strains at fixed positions and along fixed directions through physical connections to external readout devices. Such sensors provide a relatively coarse sampling of the substrate's strain field and their presence can disrupt the function of the surface being monitored. Here we demonstrate a novel noncontact method for strain monitoring based on the spectral properties of single-walled carbon nanotubes (SWCNTs). In our method, SWCNTs are unobtrusively embedded in a thin polymeric coating applied to the substrate of interest. Strain in the substrate is transmitted through the coating, deforming the embedded nanotubes and causing predictable changes in their electronic structure. These changes are measured optically, without physical contact, as strain-induced spectral shifts of the characteristic SWCNT near-IR fluorescence peaks. Substrate strains can be quantitatively deduced at any location and along any direction by positioning the excitation beam and orienting its polarization plane. The use of such "strain paint" containing nanoscale sensors promises structural health monitoring with improved simplicity and versatility.

Single-walled carbon nanotubes are a family of highly elongated tubular structures composed of carbon atoms covalently bonded into specific ordered forms. Each form has a well-defined diameter and roll-up angle and is uniquely labeled by a pair of integers, (n,m).[1] Among the remarkable properties of SWCNTs are their well-defined spectral transitions that vary systematically with physical structure,[2] reflecting the quantum confinement of π-electrons perpendicular to the tube axis. Most SWCNT structural species are semiconducting and show robust photoluminescence (fluorescence emission) at distinct near-IR wavelengths corresponding to their semiconducting band gaps.[2−4]

It is known from theory and experiment that axial stretching or compression of SWCNTs causes predictable changes in electronic structure that systematically shift their spectral transitions.[5−11] Previous studies on individual nanotubes have confirmed that these shifts occur in opposite directions for "mod 1" and "mod 2" nanotubes (for which mod $(n - m, 3)$ = 1 or 2), and that the magnitudes of the spectral shifts are proportional to $\cos(3\theta)$, where θ is the nanotube roll-up angle. These shifts in SWCNT fluorescence spectra are large enough to reveal axial strains below 0.1%, suggesting the possibility of a practical noncontact optical method to measure strains in large-scale objects using embedded SWCNTs as the sensors. This approach would represent an attractive alternative to carbon nanotube-based sensors involving strain-induced changes in electrical transport properties or Raman spectra,[12−15] because fluorescence spectroscopy requires no electrical connections and provides stronger signals and faster data acquisition than Raman.

In the scheme described here, the structural element of interest is coated with a thin polymeric film containing dilute individualized SWCNTs. If the coating adheres strongly to the substrate and to the embedded nanotubes, then strain in the coating will match that of the substrate, and embedded nanotubes will be axially deformed by the spatial projection of

Received: March 14, 2012
Revised: May 26, 2012

the coating strain along the nanotube axis. The nanotube strain at a position of interest can be quantitatively monitored by irradiating the surface with a visible laser of suitable wavelength and capturing the resulting near-IR fluorescence for spectral interpretation.

Methods. Raw SWCNTs grown in the Rice University HiPco reactor were weighed and added to a commercial exterior varnish (Minwax Helmsman 350 VOC Spar Urethane) at a weight percent of approximately 0.02%. The mixture was tip ultrasonicated at a power of about 10 W (15 s on, 15 s off duty cycle) for 10 to 30 min until the SWCNTs appeared thoroughly dispersed in the polymer. The SWCNT-polyurethane mixture was then spin-coated onto a PMMA substrate ($75 \times 25 \times 6$ mm) that had been surface-roughened using a fine sandpaper to improve adhesion and allowed to dry under ambient conditions. Spin coating was repeated until the SWCNT fluorescence emission from the surface coat was conveniently intense, and then the sample was cured for one to two weeks at room temperature prior to measurements. (We observed that the time needed for proper curing increased directly with the film thickness.) Final coating thicknesses were approximately 25 μm.

The sample was subjected to strain using a custom built four-point bending jig. Strain in the nanocomposite film close to the focus of the interrogating laser was measured by a resistive foil strain gage affixed to the film. Strain in the PMMA bar was measured using a second strain gage mounted at the corresponding location on the opposite surface of the PMMA bar. We monitored readings from the gages in real time to check for any relaxation of the polymer surface. The applied strain (measured on the PMMA bar) and strain in the polymer film were found to be nearly equal for thin polymer layers prepared by spin coating. Our bending jig was manually adjusted to give strain increments of 0.05% during loading and unloading.

SWCNT fluorescence was excited with polarized 660 nm light from a 70 mW, circularized-beam diode laser (PTI model PPM80). As shown in Figure 1a, the laser beam was passed through a Schott KG3 filter to remove near-IR components and a half-wave plate to allow adjustment of its polarization plane. It was then focused onto the sample with a 30 mm focal length lens. Sample fluorescence was collected either in the forward direction, after passing through the transparent substrate, or in the backward direction, as in Figure 1a. The emission passed through an 850 nm long-pass filter to block stray excitation light and was then coupled into a multimode optical fiber that terminated at the entrance slit of a near-IR spectrometer (CVI SM302) equipped with a thermoelectrically cooled InGaAs multichannel detector. We typically used spectral integration times of 1 s and averaged 10 spectra per acquisition. The peak fluorescence wavelengths of (7,5) and (7,6) SWCNTs in the film were found by separately fitting local Gaussian functions to the emission features near 1040 and 1140 nm. Spatial resolution in this method is equal to the size of the excitation beam at the surface, which was approximately 100 μm in this study. We verified the reproducibility of results using independently prepared samples.

Results and Discussion. We made a series of measurements with the samples and methods described above to demonstrate the feasibility of noncontact strain measurement using films with randomly oriented, structurally unsorted SWCNTs. Figure 2 compares typical SWCNT emission spectra measured from the substrate surface when unstrained and when strained to 0.55% (in tension) in a direction parallel to the polarization axis of the excitation laser. It can be seen from the insets that the peaks attributed mainly to (7,5) and (7,6)

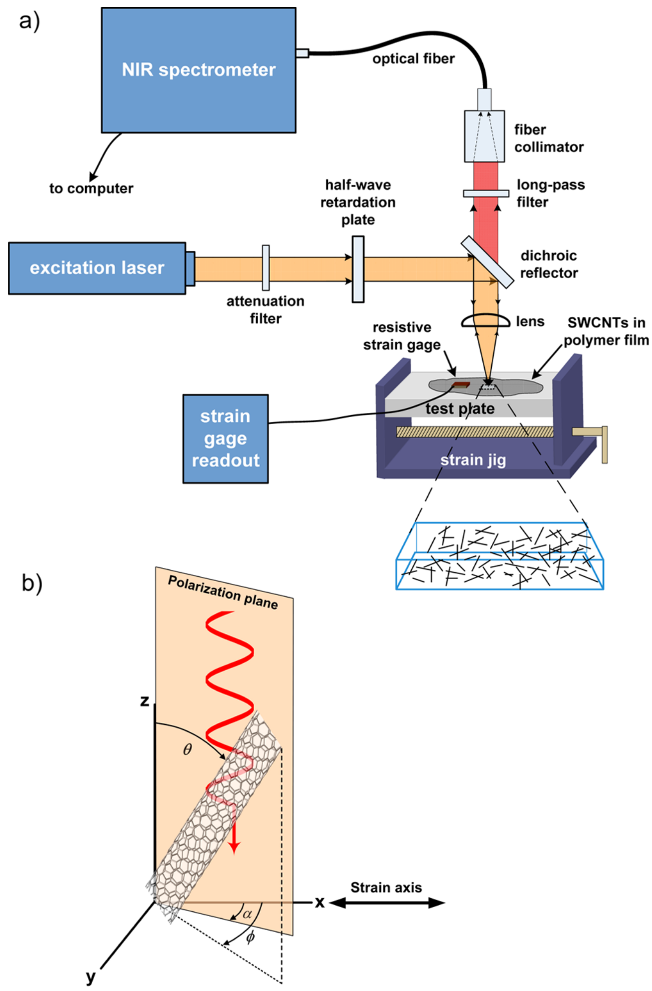

Figure 1. Schematic diagrams of (a) the experimental apparatus and (b) angle definitions.

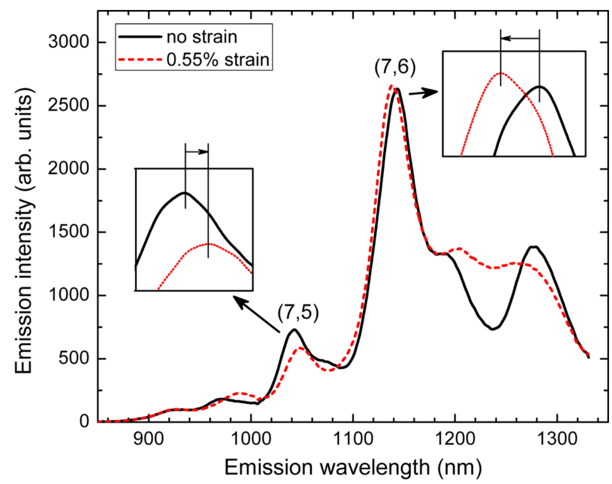

Figure 2. Changes in "strain paint" emission spectrum with applied strain. Emission spectra are shown for applied substrate strains of 0% (black solid line) and 0.55% (red dashed line). Insets illustrate the opposite shifts in peak positions for features dominated by (7,5) and (7,6) SWCNTs.

SWCNTs shift in opposite directions with strain, as is expected because (7,5) is a mod 2 nanotube whereas (7,6) is mod 1. We exploited this effect by tracking the difference between (7,6) and (7,5) peak wavelengths as the test plate was loaded and then unloaded. This differential shift measurement is nearly insensitive to global emission shifts caused by environmental changes and provides higher sensitivity to strain than measurement of either individual peak position alone. Our results (Figure 3) show linear dependences during loading and unloading with slopes of approximately 17.2 nm/% and an average hysteresis corresponding to 0.04% strain. At high strain values, we would expect nonlinearities and large irreversibilities similar to those observed in single-nanotube studies, caused by slippage of SWCNTs within the polymer film.[9] However, the small stable hysteresis seen in Figure 3 instead appears due to mechanical relaxation of the strained polymer film, which was approximately 20 μm thick. This effect should be reduced in films that are thinner or are prepared by more refined methods.

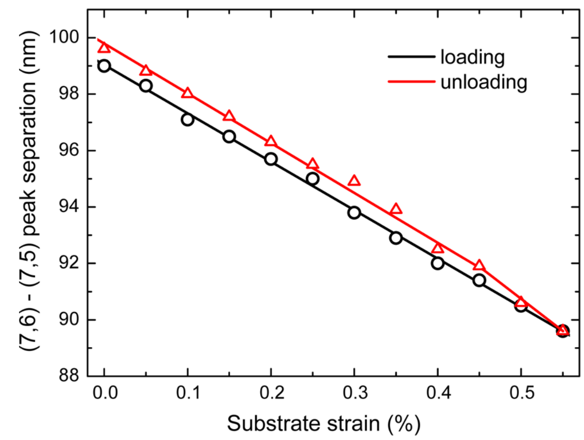

Figure 3. Strain variation of differential spectral shift. The difference in peak emission wavelengths of (7,6) and (7,5) nanotubes in a polymeric coating is plotted versus strain in the substrate, as measured with a resistive strain gage. Black circles show data measured with increasing strain; red triangles were measured with decreasing strain. Straight lines show linear best fits to the data.

When linearly polarized light is used to irradiate the coated surface, emission will be strongest for those nanotubes aligned along the polarization axis, because the dominant nanotube spectral transitions are highly anisotropic.[16−18] We measured the dependence of the (7,6) − (7,5) peak separation on polarization angle of the excitation laser relative to the applied strain axis with fixed strain (Figure 4). These data can be fit well by the function

$$\Delta\lambda = A\cos^2(\alpha - \alpha_0) + C \tag{1}$$

where α is the laboratory angle of the laser polarization axis, α_0 is the laboratory angle of the fixed strain axis, C is the (7,6) − (7,5) peak separation with no strain, and A is an amplitude factor equal to the peak-to-valley difference in Figure 4. The 0.5% fit shown was computed with $A = -8.4$ nm, $\alpha_0 = -1.9°$, and $C = 98.7$ nm. The large modulation amplitude confirms that our method can selectively resolve and measure strains along different directions of a substrate. If necessary, directional selectivity can be further increased by using polarized detection in addition to polarized excitation.

In practical implementations of this noncontact strain sensing method, properties of the polymeric film material will be important. The material must not strongly attenuate the red and near-IR wavelengths of nanotube excitation and emission transitions and must not significantly quench the intrinsic fluorescence of embedded SWCNTs. It also needs to support dispersions of individualized SWCNTs, show strong interfacial adhesion, and provide good mechanical and environmental durability. Our studies to date have found a commercial polyurethane-based varnish to be a promising material for strain paint films, but additional research will be needed to identify optimal formulations. Properties of the SWCNTs suspended in the film also affect the performance of our method. The nanotubes should be nearly pristine and unbundled to give bright near-IR fluorescence, and those specific (n,m) species used in the spectral analysis should be relatively abundant. Ideal SWCNT formulations could be prepared by enriching the desired (n,m) species through sorting methods such as density gradient ultracentrifugation.[19,20]

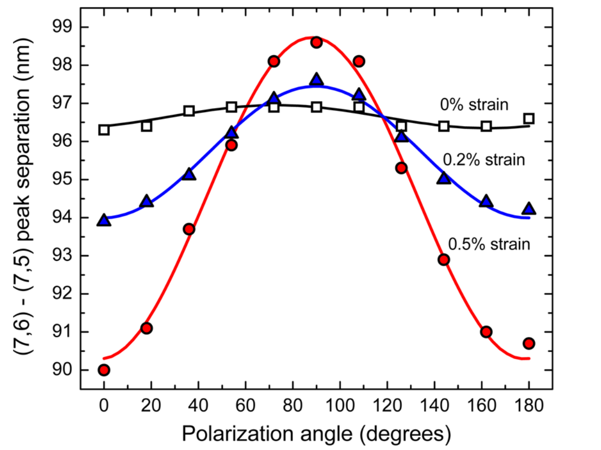

Figure 4. Polarization selectivity of differential spectral shift. The difference in peak emission wavelengths of (7,6) and (7,5) nanotubes in a polymeric coating is plotted against the angle between the axes of applied strain and excitation laser polarization. Applied strain magnitudes were 0 (open squares), 0.2% (triangles), and 0.5% (circles). The solid curves show best fits to the data using the function in eq 1.

In contrast to our prior study of individual SWCNTs in a strained polymer,[9] each spectral measurement on the coated test plate probes an ensemble of embedded SWCNTs that have random in-plane angles ϕ (Figure 1a). The distribution in polar angle θ is not known a priori, because it might vary from a uniform (random) distribution to a delta function at $\theta = 90°$ (if shrinkage of the polymer film during curing forces SWCNTs to lie parallel to the substrate surface). We can write the orientational distribution function as $f(\theta,\phi) = (1/2\pi)f(\theta)$. Consider an individual SWCNT in the film (Figure 1b). The relative probability that it will absorb light from a plane-polarized excitation beam propagating along the z-axis with the polarization plane intersecting the x−y plane at an angle α to the x-axis is $\sin^2(\theta)\cos^2(\phi - \alpha)$. For strain applied parallel to the x-axis, the resulting spectral shift of the nanotube fluorescence, Δ, will have an angular dependence $\Delta(\theta,\phi,\alpha) = \Delta_{max}(\cos^2\beta - \eta\sin^2\beta)$, where Δ_{max} is the shift for that (n,m) species when the strain is applied parallel to the tube axis, $\beta = \arccos(\sin\theta\cos\phi\cos\alpha + \sin\theta\sin\phi\sin\alpha)$ is the angle between the nanotube axis and the strain axis, and η is Poisson's ratio for the host polymer. The two terms in $\Delta(\theta,\phi,\alpha)$ express nanotube axial strains caused by the host's direct deformation along the x-axis and indirect opposite deformation (Poisson effect) along the transverse directions. The emission spectrum from each (n,m) species will be a superposition of peaks from nanotubes with various orientations and corresponding variations in intensities and strain-induced spectral shifts. We can express $S(\Delta)$, the intensity-weighted distribution of spectral shifts, as

$$S(\Delta) = \int_0^{2\pi} \int_0^{\pi} f(\theta, \phi)\Delta(\theta, \phi, \alpha)\sin^2(\theta)\cos^2(\phi - \alpha)\sin(\theta)\mathrm{d}\theta\mathrm{d}\phi \tag{2}$$

or

$$S(\Delta) = \frac{1}{2\pi} \int_0^{2\pi} \int_0^{\pi} f(\theta)\Delta(\theta, \phi, \alpha)\sin^3(\theta)\cos^2(\phi - \alpha)\mathrm{d}\theta\mathrm{d}\phi \tag{3}$$

This relation describes how an ensemble of orientationally distributed SWCNTs in a strained environment gives an emission spectrum that is broadened and less shifted in peak position than the same nanotubes aligned parallel to the strain axis and parallel to the surface. By evaluating eq 3 using the Δ_{max} values found from theory and prior experiments and comparing the result with the empirical slope in Figure 3, we deduce that $f(\theta)$, the distribution of polar angles, has a strong maximum near $\theta = 90°$. This implies that SWCNTs are preferentially aligned parallel to the surface through application and curing of the polymer film.

Despite the formal complexities discussed above in using first principles to deduce strains from spectroscopic data on ensembles of orientationally diverse SWCNT samples, the data in Figures 3 and 4 demonstrate sensitivity, precision, and directional resolution that are suitable for practical applications. Our method allows mapping a strain field over a wide area simply by moving the optical system to each point of interest and capturing emission spectra for several polarization settings of the excitation beam. The grid used in such strain mapping can be as coarse or fine as desired (limited only by size of the focused excitation beam), because the SWCNT sensors are homogeneous throughout the coating. Absolute strain values can be found by applying empirical calibrations determined for the relevant strain paint formulations and application methods. Although the present results have been obtained with laboratory instrumentation, it seems likely that the necessary optical and computer hardware can be integrated into a field-portable strain reader that could capture and analyze spectra even faster than the few seconds used to acquire data points in this study.

In practical applications, the polymer coatings used to embed the SWCNTs can provide environmental protection and mechanical strengthening in addition to sensing. Such multi-functional strain paints or smart skins might be used to coat the fuselage, wings, or tail in new aircraft, such as the Boeing 787, that employ components made from carbon fiber reinforced polymers (CFRP). The smart skin coating could also sense strain in retrofitted buildings and bridges containing beams or columns reinforced with CFRP. As an example, smart skin-coated CFRP reinforcing fabric or fibers would be used to wrap the concrete columns of large bridges to enhance their shear strength for earthquake protection. The results presented here demonstrate the potential of noncontact strain sensing only in static or monotonic applications. However, it may be possible to develop variants of the method that deduce strain much more quickly by capturing and analyzing only a few selected spectral channels of SWCNT fluorescence. If successful, this would allow extension to dynamic applications. In summary, we anticipate that our sensing approach will enable practical noncontact strain measurements for improved structural health monitoring in aerospace and civil engineering.

AUTHOR INFORMATION

Corresponding Author

*E-mail: weisman@rice.edu.

Notes

The authors declare no competing financial interest.

ACKNOWLEDGMENTS

Authors P.A.W., S.M.B., and R.B.W. are grateful to the National Science Foundation (Grant CHE-1112374) and the Welch Foundation (Grant C-0807) for support of this work. V.S.M. and S.N. acknowledge support by the Air Force Research Laboratory (AFRL fund FA8650-05-D-5807) under the Materials and Manufacturing Directorate (B. Maruyama, Program Manager) and by ICAM at Rice University. We thank J. Streit for film thickness measurements.

REFERENCES

(1) Reich, S.; Thomsen, C.; Maultzsch, J. *Carbon Nanotubes: Basic Concepts and Physical Properties*; Wiley-VCH: Weinheim, 2004.

(2) Bachilo, S. M.; Strano, M. S.; Kittrell, C.; Hauge, R. H.; Smalley, R. E.; Weisman, R. B. *Science* **2002**, *298*, 2361−2366.

(3) O'Connell, M. J.; Bachilo, S. M.; Huffman, C. B.; Moore, V.; Strano, M. S.; Haroz, E.; Rialon, K.; Boul, P. J.; Noon, W. H.; Kittrell, C.; Ma, J.; Hauge, R. H.; Weisman, R. B.; Smalley, R. E. *Science* **2002**, *297*, 593−596.

(4) Weisman, R. B.; Bachilo, S. M. *Nano Lett.* **2003**, *3*, 1235−1238.

(5) Yang, L.; Han, J. *Phys. Rev. Lett.* **2000**, *85*, 154−157.

(6) Minot, E. D.; Yaish, Y.; Sazonova, V.; Park, J.-Y.; Brink, M.; McEuen, P. L. *Phys. Rev. Lett.* **2003**, *90*, 156401−1−156401−4.

(7) Li, L.-J.; Nicholas, R. J.; Deacon, R. S.; Shields, P. A. *Phys. Rev. Lett.* **2004**, *93*, 156104−1−156104−4.

(8) Maki, H.; Sato, T.; Ishibashi, K. *Nano Lett.* **2007**, *7*, 890−895.

(9) Leeuw, T. K.; Tsyboulski, D. A.; Nikolaev, P. N.; Bachilo, S. M.; Arepalli, S.; Weisman, R. B. *Nano Lett.* **2008**, *8*, 826−831.

(10) Huang, M. Y.; Wu, Y.; Chandra, B.; Yan, H.; Shan, Y.; Heinz, T. F.; Hone, J. *Phys. Rev. Lett.* **2008**, *100*, 136803−1−136803−4.

(11) Valavala, P. K.; Banyai, D.; Seel, M.; Pati, R. *Phys. Rev. B* **2008**, *78*, 235430−1−235430−6.

(12) Li, Z.; Dharap, P.; Nagarajaiah, S.; Barrera, E. V.; Kim, J. D. *Adv. Mater.* **2004**, *16*, 640−643.

(13) Dharap, P.; Li, Z.; Nagarajaiah, S.; Barrera, E. V. *Nanotechnology* **2004**, *15*, 379−382.

(14) Vemuru, S. M.; Wahi, R.; Nagarajaiah, S.; Ajayan, P. M. *J. Strain Analysis* **2009**, *44*, 555−562.

(15) Srivastava, R. K.; Vemuru, V. S. M.; Zeng, Y.; Vajtai, R.; Nagarajaiah, S.; Ajayan, P. M.; Srivastava, A. *Carbon* **2011**, *49*, 3928−3936.

(16) Miyauchi, Y.; Oba, M.; Maruyama, S. *Phys. Rev. B* **2006**, *74*, 205440-1−205440-6.

(17) Lefebvre, J.; Fraser, J. M.; Finnie, P.; Homma, Y. *Phys. Rev. B* **2004**, *69*, 075403−1−075403−5.

(18) Casey, J. P.; Bachilo, S. M.; Moran, C. H.; Weisman, R. B. *ACS Nano* **2008**, *2*, 1738−1746.

(19) Arnold, M. S.; Green, A. A.; Hulvat, J. F.; Stupp, S. I.; Hersam, M. C. *Nat. Nanotechnol.* **2006**, *1*, 60−65.

(20) Ghosh, S.; Bachilo, S. M.; Weisman, R. B. *Nat. Nanotechnol.* **2010**, *5*, 443−450.